Nominal GPS Signal Deformations: 10 years of WAAS Signal Quality Monitoring

R. Eric Phelts, Todd Walter, Stanford University:
Rhiannon Sanchez, *Federal Aviation Administration*

ABSTRACT

Approximately 10 years of continuous WAAS signal quality monitoring (SQM) measurements have been collected. Numerous changes to the GPS satellite constellation, WAAS ground system, and user receiver configurations have occurred during that time. A number of anomalous signal deformation events have also been cataloged on L1 since 2009. Despite these various changes, WAAS SQM data can be used to assess the stability and evolution of nominal signal deformations of the L1 C/A code signals from the GPS satellites. In addition, the more recent availability of L5 SQM data and the addition of GPS Block III SVs allows comparisons to the original L1 algorithm and predictions for future nominal L5 characteristics. It is shown that WAAS SQM measurements remain sensitive to changes in nominal signal deformations. Also, while the limits of nominal deformations appear quite stable and signal anomalies tend to be rare, unexpected events can and do occur. Finally, though GPS Block III SVs have dissimilar signal characteristics to previous block types, the maximum nominal range biases on L1 continue to be well-bounded by the threat model and minimum range error limits required to guarantee integrity for single-frequency WAAS aviation users. It is anticipated this will hold true for future dual-frequency WAAS users as well.

INTRODUCTION

The Wide Area Augmentation System (WAAS) uses a distributed network of ground reference receivers to provide corrections and navigation integrity for aviation users of GPS over most of North America. Its receivers monitor the GPS signals to correct errors and detect potential integrity threats. The WAAS signal quality monitor (SQM) algorithm is designed to detect anomalous distortions of signal correlation peaks to prevent them from causing hazardously large range errors.

Originally, the WAAS SQM was only required to mitigate a subset of the signal deformation threats of concern on L1 C/A. The first ground reference receivers had minimal correlators per channel for correlation peak monitoring, so SQM capability was limited to detecting significant shifts of correlation peaks, using a code-carrier coherence monitor [1]. True, multi-correlator SQM receivers were not fielded and fully operating until 2008. This enabled WAAS to protect aviation users of L1 C/A code against the full range of deformation threats and help to meet the integrity requirements to support flight operations with more stringent integrity requirements. (The full signal deformation threat model is summarized in [2] and described more completely in [3].)

Since 2008, the SQM detection algorithms have been refined and the integrity analyses updated [4]. Between 2015 and 2017, the deformation monitor receivers were upgraded to include more detection sensitivity (i.e., wider bandwidth) and capability to track L5 signals. More recently, algorithms have been developed to enable WAAS to monitor L5 signals. Additional correlation peak monitor metrics have been proposed and their effectiveness assessed at mitigating the threat model for dual-frequency WAAS users while not increasing the likelihood of false monitor trips. In addition, since 2018, GPS-III space vehicles (SVs) are being continually added to the GPS constellation. Accordingly, the existing monitor has thus far successfully integrated those signals, despite their somewhat different signal characteristics than those from previous GPS Block types. [5]

Recent offline analysis tools combined with historical WAAS SQM data now provide the capability to analyze nominal GPS signal characteristics in more detail based on their monitor responses. And past detection capabilities and algorithms can be compared to current and future ones. Further, the proposed future algorithm modifications can now be evaluated and tuned based on past (nominal and anomalous) signal data both for L1 and L5 signals. And valuable insights can be gained from analyzing the monitor data over the past decade, provided the various changes to GPS and WAAS are considered.

TERMINOLOGY

In this paper, nominal *monitor biases* will refer to the (time-averaged) WAAS SQM detection metrics that persist below the minimum detection threshold without causing the monitor to trip. They are a measure of the dissimilarity of the received signal correlation peaks as measured by the monitor metrics. Nominal *range biases* will refer to the user receiver range errors caused the inherent dissimilarity of the signal correlation peaks. They are related to the magnitudes of the monitor biases. Signal *anomalies* (or *anomalous signals*) will refer to temporary signal events that may or may not cause monitor trips. They can affect both monitor biases and can cause range biases.

WAAS SQM OVERVIEW: (2008-Present)

Signals

WAAS SQM was originally designed to operate on L1 C/A code. It has used multi-correlator SQM receivers to do this since 2008. Since the reference receiver upgrade in mid-2016, WAAS has had the capability to track and monitor the L5 signal, but the system WAAS has not yet been certified for dual-frequency use.

L5-capable GPS SVs began with the launch of the Block IIF-1 in mid-2010. And, as of the writing of this paper, there are 17 L5-capable GPS satellites (12 Block IIF SVs and five Block III SVs) on orbit. The L5 signal is 10x wider bandwidth and requires different processing by the monitor receivers. The development of aviation receiver requirements and algorithms for tracking and processing L5—necessary steps toward certifying WAAS for dual frequency use—has been ongoing in some form for over 10 years.

The WAAS SQM algorithm and processing required for L5 will remain largely the same, however the integrity requirements for dual-frequency (L1-L5) WAAS aviation users are different. It follows that monitor detection requirements have increased. And the design and performance must be assessed using the real-world monitor performance of the signals. For example, the best detection capability (e.g., minimum thresholds theoretically achievable) is necessarily limited by the nominal noise and signal biases inherent on the signals.

GPS Block Types

GPS Bock III SVs implement more modern signal generation methods than previous Block types. The signals are in fact closer to ideal [5], but this means their signals may differ more substantially from the others. In other words. Block III satellite signals are expected to appear more nominally deformed relative to most of the others.

The current WAAS monitor has to integrate these (L1) signals without causing too many false alarms or trips. The future monitor has to account for potential variations between L5 signals from Block IIIs vs Block IIFs. These variations appear as nominal monitor biases and may limit the sensitivity of the monitor.

Monitor Receivers

WAAS SQM monitors for correlation peak distortions using a network of 114 reference receivers located at 38 reference stations distributed throughout the U.S. From 2008 to mid-2015 each of the receivers was capable of monitoring L1 C/A code (only). Each had a 18 MHz front-end bandwidth and used a narrow correlator (0.1-chip, or ~100ns), early-minus-late (EML) discriminator. Between 2015 and 2017 those reference/monitor receivers were replaced with receivers capable of tracking and monitoring L5 signals. The L5 discriminator remains similar to the one for L1 (~100 ns, early-minus-late). And the front-end bandwidth (for both L1 and L5) was widened to 24 MHz.

WAAS reference receivers measure the correlation peaks on both L1 and L5 with a total of 9 correlator outputs, including the three (Early, Late, and Prompt) used for forming the Early-Late discriminator. The correlator offsets on L1 vary from -100ns to +100ns (relative to Prompt) at 25 ns increments. On L5, they vary from -50 ns to +50 ns at an average of ~12 ns increments.

Note that the correlator measurements are only available when the receiver is phase-locked so only the in-phase (I) measurements are used for detection considered; quadrature (Q) measurements are ignored.

Detection Metrics

For L1 signals WAAS currently implements a total of 4 detection metrics—vectors that form linear combinations of the 9 correlator outputs—which are found by the method described in [6]. These were computed specific to the model of the original monitor receiver filter and models of the deformation threats. They were not updated after the receivers were upgraded from 18 MHz to 24 MHz, however since predicted detection performance remained satisfactory.

For dual-frequency operation, WAAS proposes to employ an additional 8 metrics on L1 and the same 8 metrics on L5. These are simple pairwise differences of adjacent correlator outputs designed to estimate the code chip shape as described in [7]. Accordingly, in the future, WAAS will implement a total of 12 detection metrics on L1 ($_{\{L1\}}M=12$), and a total of 8 on L5 ($_{\{L5\}}M=8$).

L1 and L5 signals and metrics will be processed in parallel. The L5 metric processing has yet not been implemented in WAAS SQM but algorithm upgrades are in the development and prototyping stages. This paper contains some early results from these efforts using historical SQM data from as recently as June 2021.

In this paper, nominal *monitor biases* will refer to the (time-averaged) WAAS SQM detection metrics that persist below the minimum detection threshold without causing the monitor to trip. They are a measure of the inherent dissimilarity of the signal correlation peaks as measured by the monitor metrics.

Type Biases

For L1 C/A code, not all correlation peaks have the same slope [2]. In fact, there are three possible ideal C/A code correlation peak slopes. These correspond to the three PRN types. (There is only one ideal peak slope/PRN type for L5 PRNs.) Several C/A code PRNs are narrower (i.e., have greater slope), a few others are wider (i.e., have a slightly reduced slope) than normal. This results in metric biases that are completely deterministic for known PRN codes. Provided when the filter characterization is known, it can be computed and removed.

Using the receiver-specific filter characterizations, the analytical approach has traditionally been employed by WAAS for estimating the type biases for the four metrics on L1. (The calibration was done twice—once for the receivers in 2008, a second time for the receivers after the upgrade in between 2015 and 2017.) However, type biases corresponding to several of the additional 8 chip-shape metrics on L1 appear more sensitive to the nominal distortions on some signals. And empirically-estimated PRN type biases provide better estimates and result in smaller nominal monitor metric biases at the output. (See Equation 9.)

Note that this estimation is still required only once for a given monitor receiver design. PRN type bias estimates have been found to be very stable over time. (The William J. Hughes FAA Technical Center has measured and included PRN type bias estimates in its quarterly WAAS PAN reports since 2008. [8])

User Receiver Configurations

The range of allowed receiver design parameters determines the maximum range error that WAAS must protect against. In general, the more dissimilar any particular user receiver configuration is to the WAAS reference receivers, the larger the expected differential range errors are from signal deformations. As a result, the constraints on receiver discriminator type, correlator spacing, front-end bandwidth, and group delay can significantly affect the final monitor design and effectiveness.

Since 2009, WAAS SQM has protected the L1 early-minus-late receiver configurations indicated by the darker blue areas in Figure 1a. (So-called "double-delta" discriminator receivers are also protected, but are not shown here. And precise specifications on all these receiver discriminators, filters, etc. is given in [9].) After the WAAS reference receiver upgrade in mid-2016, a narrow range of discriminators (0.08 to 0.12 chip EML correlator spacings) in the 20 to 24 MHz BW region shown in light blue was included for L1 users as well.

Figure 1b shows how L1-L5 aviation receivers will be constrained to a much narrower range of designs. This will reduce the differences between the reference and user receivers and thereby limit the maximum differential range biases. This reduction is needed because, for dual-frequency users, biases on L1 and L5 will be amplified by the formation of the dual-frequency combination by factors of 2.26 and 1.26, respectively. [7]
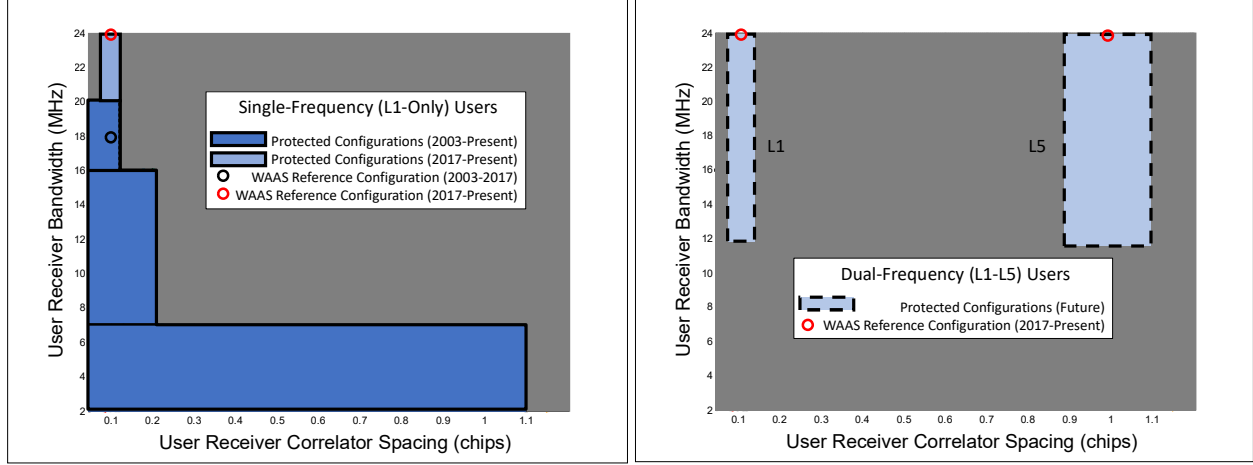
Figure 1a. (Left) Current L1-only user receiver design space for early minus late receivers.
Figure 1b. (Right) Proposed L1-L5 user receiver design space for early-minus-late discriminators

In this paper, nominal *range biases* will refer to the user receiver range errors caused the inherent dissimilarity of the signal correlation peaks. They are related to the magnitudes of the monitor biases.

Tradeoffs

Improvements to the monitor receiver hardware improve detection sensitivity and additional metrics provide improved threat mitigation capability. However, this sensitivity can increase the nominal monitor biases and raise the minimum achievable monitor threshold for low false alarm probability.

The addition of L5 enables dual-frequency operations, which provides smaller range error limits and greater capability for WAAS users. And reduced allowable user L1-L5 receiver design space reduces largest differential user range errors dur to signal deformation. However, dual-frequency processing amplifies any range biases and errors on each frequency.

Newer, better satellites strengthen the GPS constellation and the newer signal generation techniques will improve overall signal quality over the long term. This should ultimately translate to smaller nominal signal biases. In the short term, however, because the newer SVs are relatively few, their signals may introduce small nominal biases into the position solution due to their differences from the signals from older SVs.

WAAS SQM ALGORITHM (L1: 2008-2021; L1-L5: 2022-)

The basics of the processing algorithm procedure has remained largely unchanged since 2008. However, to account for additional metrics on L1 and L5, the algorithm outlined in [2] has been updated.

The dual-frequency monitor will process both L1 and L5 signals independently and in parallel. A threshold trip on either signal will cause the system to flag the SV as "Do Not Use" so WAAS users know to exclude it from their position solution. Note that the probability of a simultaneous signal deformation anomalous event on both L1 and L5 is presumed to be negligible. (This modifies the assumptions of [7], where a simultaneous threat on both signals was analyzed.)

The general WAAS SQM processing procedure for GPS L1 and L5 procedure follows. (Exception handling and other operational system details have been omitted for conciseness and clarity.)

Note that in all subsequent equations, Ln represents either frequency L1 or L5, i represents the satellite, j refers to the receiver, and m is the metric under consideration. And, for clarity, $1 \leq m \leq 8$ will identify the new, proposed chip-shape metrics on both L1 and L5. And $9 \leq m \leq 12$ will identify original (and current) metrics implemented on L1 only.

<u>Procedure</u>

1. *Normalize and Filter Correlator Outputs*

For C/A code, the nine in-phase correlator measurements, I_x, x = 1 to 9 correspond to code offsets symmetrically distributed relative to Prompt, P (P= I_5). (The Prompt by definition, has a relative offset of 0 and after normalization, equals unity). Each correlator measurement I_x is then smoothed with a first order filter with time constant $F = 50$ seconds.

$$_{(Ln)}r^i_{j,x}(t) = \frac{1}{F_r}\left[\frac{_{(Ln)}I^i_{j,x}(t)}{_{(Ln)}P^i_j(t)}\right] + \frac{F_r-1}{F_r}\left[_{(Ln)}r^i_x(t-1)\right] \tag{1}$$

In the above equation, Ln implies either signal L1 or L5.

2. *Compute Detection Metrics*

The signal deformation detection metrics are formed by a linear combination of those correlator outputs on the ith satellite for each metric, m this is detection metric is described by

$$_{(Ln)}d^i_{j,m}(t) = \sum_{x=1}^9 {}_{(Ln)}\alpha_{m,x}\left(_{(Ln)}r^i_x(t)\right) = \left[_{(Ln)}\bar{r}^i_j(t)\right]^T {}_{(Ln)}\bar{\alpha}_m \tag{2}$$

Where $_{(Ln)}\bar{r}^i_j(t)$ and $_{(Ln)}\bar{\alpha}_m$ are each 9x1 column vectors of the normalized, filtered correlator outputs and the scalar multiples of those outputs, respectively

For L5 and L1 and m = 1 to 8, the elements of the chip shape metric vectors, $_{(L1)}\bar{\alpha}_m$ and $_{(L5)}\bar{\alpha}_m$, are defined by

$$\begin{array}{ll} m \le 8, x = m & \alpha_{m,x} = 1, \\ m \le 8, x = m+1 & \alpha_{m,x+1} = -1, \\ Otherwise & \alpha_{m,x} = 0 \end{array} \tag{3}$$

For L1 (only) and m = 9 to 12, the elements of $_{(L1)}\bar{\alpha}_m$ of are found by the method described in [6]. As previously stated, for L1, the total number of metrics $_{(L1)}M$ = 12 and for L5, the total number of metrics $_{(L5)}M$ = 8.

3. *Estimate and Remove Inter-Receiver Biases* (*IRBs*)

Each monitor receiver introduces a small receiver- dependent (and metric-dependent) bias that must be removed. This inter-receiver bias (IRB) is estimated slowly-varying and is estimated each receiver and metric by an additional first-order smoothing filter with time constant, F_{IRB} (where $F_{IRB}>>F_r$). That is averaged across each SV i tracked by each receiver j. (Note IRBs for metrics applied to geostationary (GEO) satellites are treated separately because of additional biases introduced by their signal generation filters [10]. These equations are not included here.)

$$\left[_{(Ln)}\hat{b}^i_{j,m}(t)\right] = {}_{(Ln)}d^i_{j,m}(t) - \sum_{j=1}^{(Ln)J^i_m} {}_{(Ln)}w^i_{j,m}\left[_{(Ln)}d^i_{j,m}(t)\right] \tag{4}$$

where $_{(Ln)}w^i_{j,m}$ is a weighting factor of the measurements and is a function of the standard deviations of the previously filtered metrics $_{Ln}d^i_{j,m}(t)$.

$$_{(Ln)}w^i_{j,m} = \frac{\frac{1}{\left[_{(Ln)}\sigma^i_{j,m}(\theta^i_j)\right]^2}}{\sum_{j=1}^{J^i_m}\left\{\frac{1}{\left[_{(Ln)}\sigma^i_{j,m}(\theta^i_j)\right]^2}\right\}} \tag{5}$$

In the above equation, $_{(Ln)}\sigma^i_{j,m}(\theta^i_j)$ is an *a priori* elevation angle-dependent standard deviation function of the measurements. It is specific to each metric $_{(Ln)}m$, for applied to receiver j, and viewing satellite i viewed at an elevation angle θ.

The IRB per-receiver is then given by

$$_{(Ln)}^{GPS}b_{j,m}(t) = \frac{1}{N_{GPS}} \sum_{i=1}^{N_{GPS}} {}_{(Ln)}b^i_{j,m}(t) \tag{6}$$

where

$$_{(Ln)}b^i_{j,m}(t) = \frac{1}{F_{IRB}}\left[{}_{(Ln)}\hat{b}^i_{j,m}(t)\right] + \frac{F_{IRB}-1}{F_{IRB}}\left[{}_{(Ln)}\hat{b}^i_{j,m}(t-1)\right] \tag{7}$$

And the IRBs are removed for each SV according to

$$_{(Ln)}D^i_m(t) = \sum_{j=1}^{{}^{(Ln)}J^i_m} {}_{(Ln)}w^i_{j,m}\left[{}_{(Ln)}d^i_{j,m}(t) - {}_{(Ln)}b_{j,m}(t)\right] \tag{8}$$

4.   Remove SV Type Biases

The output of Equation 8, $_{Ln}D^i_{j,m}(t)$ can averaged over several days (with no anomalies present) to compute the type biases for the three GPS PRN (correlation peak) types according to Equation 9 below.

$$_{(Ln)}B^{\zeta}_m(t) = \underset{\zeta}{\text{mean}}\left[\frac{1}{(t_Y-t_o)}\sum_{y=0}^{y=Y} {}_{(Ln)}D^i_m(t_y)\right], \; t_Y \gg t_0 \tag{9}$$

where $\zeta = 1, 2,$ and 3 for each respective C/A code PRN type. And $_{(L5)}B^1_m = {}_{(L5)}B^2_m = {}_{(L5)}B^3_m$ for L5.

$$_{(Ln)}D^i_m(t) = {}_{(Ln)}D^i_m(t) - {}_{(Ln)}B^{\zeta}_m(t) \tag{10}$$

5.   *Average Across Receivers and Median Across SVs*

The final, unbiased, receiver-averaged (unnormalized) detection metric is then referenced (adjusted) to the median metric across all SVs according to

$$_{(Ln)}D^i_{m,adj}(t) = {}_{(Ln)}D^i_m(t) - \underset{i}{\text{median}}\left({}_{(Ln)}D^i_m(t)\right) \tag{11}$$

Note the measured "ideal" signal effectively defined as the median signal across all SVs in view. In modeling analyses, however, the reference corresponds to the receiver-filtered, ideal code with no threat model distortions applied.

6.   *Normalize by Threshold and Compute Detection Test*

Equation 11 is normalized by a threshold to form detection tests for all $_{(L1)}M$ metrics on L1 and $_{(L5)}M$ metrics on L5. The maximum over all metrics on L1 and L5 is then taken. If any test exceeds unity, an alert is declared and the WAAS flag for SV i is set to "Do Not Use".

$$_{(Ln)}\Gamma^i = \underset{m}{\max}\left(\frac{\left| {}_{(Ln)}D^i_{m,adj}\right|}{{}_{(Ln)}T^i_m}\right) \tag{12}$$

where

$$_{(Ln)}T^i_m = K_{ffd} {}_{(Ln)}\sigma^i_m(\theta^i_j). \tag{13}$$

and

$$\left[{}_{(Ln)}\sigma_m^i\left(\theta_j^i\right)\right]^2 = \sum_{j=1}^{J_m^i} {}_{(Ln)}w_{j,m}^i\left\{\left[{}_{(Ln)}\sigma_{j,m}^i\left(\theta_j^i\right)\right]^2\right\} \tag{14}$$

K_{ffd} is a constant determined by the desired maximum false alarm probability of the monitor, assuming AWGN assumptions for ${}_{(Ln)}\sigma_m^i\left(\theta_j^i\right)$.

Maximum monitor sensitivity (i.e., best detection capability) occurs when the signal is well-observed by the WAAS receivers and threshold ${}_{(Ln)}T_m^i$ is minimized, ${}_{(Ln)}T_m^i = {}_{(Ln)}T_{m,\min}^i$. Accordingly, the least monitor sensitivity is when the signal is least observed and the threshold ${}_{(Ln)}T_m^i$ is maximized, ${}_{(Ln)}T_m^i = {}_{(Ln)}T_{m,maz}^i$.

WAAS SQM ANOMALOUS DEFORMATION EVENTS (2009-2021)

In this paper, signal *anomalies* (or *anomalous signals*) will refer to temporary signal events that may or may not cause monitor trips. They can affect both monitor biases and can cause range biases.

Table 1 below summarizes the known GPS signal deformation anomalies and events since 2009 on L1. (Real-time monitoring on L5 is still in development for WAAS and no anomaly information is yet known for it.) Most of these were first compiled in [11] and are described in detail in there. The current WAAS SQM (using only metrics 9-12) was online for all of these. Only one from this list, however, resulted in a monitor trip. That occurred on Jan 28, 2017 on SVN 66 (PRN 27).

Table 1 table lists one event (for July 01, 2021) that was not included in [11]. That anomaly is explored further detail at the end of this paper.

Table 1. GPS signal deformation anomalies since 2009

Date	SVN	Block Type	PRN	Monitor Trip?	Description	Source
04 to 07 Aug 2009	54	IIR	18	GBAS Only	Anomalous code distortion led to ~50 cm shift on L1 C/A. (L5 measurements not available.)	Unknown
August 2009-2010 (Test Mode)	49	01	IIR-M	None (SV Never set healthy)	Multipath-like reflection on L1 C/A caused 0 to 2m range biases depending on relative elevation angle to SV. . (L5 measurements not available.)	Internal reflection due to impedance mismatch
07 March to 08-May 2016	54	IIR	18	GBAS Only?	Anomalous code distortion on L1 C/A led to ~50 cm shift. . (L5 measurements not available.)	Unknown
31- Oct-2013	61	IIR	02	None	Anomalous Code distortion led to ~2-m shift on L1 C/A. . (L5 measurements not available.)	Power failure that impacted satellite signal amplifiers in addition to other components
July 27-29, 2016	Various [11]	Various [11]	Various [11]	None	Anomalous Code distortion led to 1.5-m shift on L1 C/A; resolved after testing ended. . (L5 measurements not obtained because WAAS receivers not L5 capable)	High P/High-C/A testing
Jan 28, 2017	66	27	IIF	YES	Unknown	High P/High-C/A testing
July 1, 2021	66	27	IIF	None	Anomalous Code distortion on L1 C/A. No effect on L5 code.	Unintentional off-nominal configuration of the L1 and L2 signals broadcast from SVN66-PRN27

WAAS SQM PERFORMANCE (2008-2021)

With knowledge of the ICAO signal deformation threat model, the WAAS reference/monitor receivers and the configurations of the user receivers, the maximum error due to satellite deformation anomalies can be computed for L1-only and L1-L5 users [7]. A curve of maximum user range error plotted as a function of the maximum monitor response can be compared to the error limits to assess the ability of the monitor to detect the threats sufficiently. The smallest error limit not exceed by the range error vs monitor curve represents the performance limit of the monitor. Smaller achievable error limits translate to greater operational capability for WAAS aviation users.

Figures 2a and 2b plot the curves for the max user differential range error as a function of the magnitude of threshold-normalized monitor metric (Equation 12). The range error limits as a function of the single-frequency differential range error index (UDREI) and dual-frequency range error index (DFREI) are plotted to show the upper-bounds on this error. These are derived from the method described in [4] and [7]. (Cases of non-differentially corrected errors do were not analyzed here.)

Figure 2a shows the progression of the monitor capability as the system was upgraded over time. In 2008 the performance barely met the criteria when the thresholds were relatively large (i.e., when the SV just coming into view of the WAAS network and observed by fewer reference stations). By 2017, after the reference receiver upgrades and additional tuning the detection capability increased and provided margin at the error bounds.

The lowest error vs monitor response curves in Figure 2a represent the cases where the maximum number of monitor receivers are observing the SV and the threshold is at a minimum (i.e., the satellite is most observed by the WAAS network). For L1, this implies $_{(L1)}T_{m,min} = {}_{(L1)}T_{m,max}/4$. These curves represent the best detection capability of the monitor and show the largest user range errors expected for threats in the model. At this level the nominal biases can be best estimated. Note that the expected range errors from signal anomalies at this level are on the order of 1.5 meters. These are well below the minimum error limit at the current WAAS UDREI floor ($UDREI_{min} = 5$).

For dual-frequency users, the error limits are smaller because ionospheric errors are assumed to be negligible. Figure 2b plots these error limits (indexed by dual-frequency range error indices, or DFREIs) for the proposed L1-L5 monitor implementation and user receiver configurations for future dual-frequency WAAS users. (See Figure 1b.) Here, the error vs monitor response curves for L1 and L5 are scaled by 2.26 and 1.26, respectively. And, based on these metrics, constraints, and assumptions, the minimum achievable DFREI is 2.

In Figure 2b, the lowest curves for $_{(L1)}T_{m,min} = {}_{(L1)}T_{m,max}/4$ and $_{(L5)}T_{m,min} = {}_{(L5)}T_{m,max}/4$, are also plotted. For L1 this minimum threshold is achievable in practice. However, for L5, the minimum threshold will likely not be permitted to go below $_{(L5)}T_{m,min} = {}_{(L5)}T_{m,max}/1.71$. The nominal variations between L5 signals from different SVs are relatively large (compared to L1). Allowing a smaller threshold on L5 would likely produce too many false alarms under nominal conditions. This is discussed further in the section entitled "Nominal Deformation Biases (2021-?)" and is shown in Figures 6a and 6b.
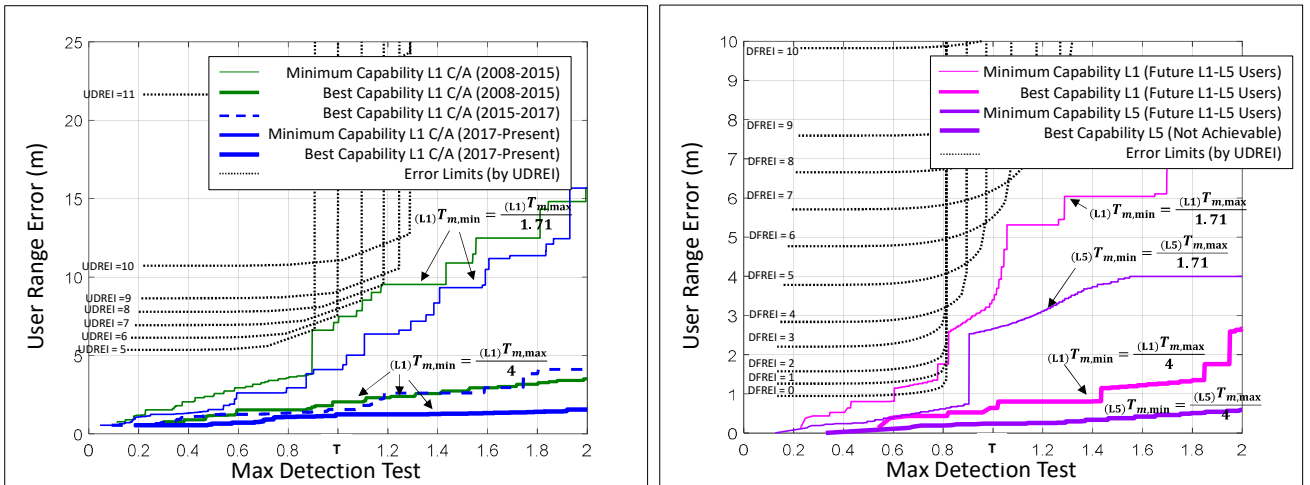

Figure 2a. (Left) L1-only user range errors as a function of monitor detection sensitivity compared to range error limits.
Figure 2b. (Right) L1-L5 user receiver design space for early-minus-late discriminators compared to range error limits

WAAS SQM NOMINAL DEFORMATION BIASES (2011-2020)

WAAS Monitor Data

Figure 3 shows the maximum of the current 4 monitor metrics $_{(L1)}\Gamma^i$ on L1 ($9 \leq m \leq 12$) at the "best" observability of each SV—i.e., the average at UDREI=5 ($_{(L1)}T_{m,min} = _{(L1)}T_{m,max}/4$) for all GPS PRNs L1 from 2011 to 2020. Results from geostationary SVs are excluded. Two of the anomaly events—SVN 62 (PRN 02) and SVN 54 (PRN 18), SVN from Table 1 are plotted to show their effect on the nominal biases as measured by the monitor. The WAAS SQM also tripped to 20% above the threshold due to a high-power testing on Jan 28, 2017 on SVN 66 (PRN 27), but the average $_{(L1)}\Gamma^i$ over that day remained relatively unchanged, so is not noticeable in this plot. Overall, the average effects in each anomalous case were notable but short-lived. The metrics have remained relatively stable over the long term.

During the upgrade of WAAS monitor receivers, which occurred between mid-2015 and mid-2016, the minimum threshold (which is mor than twice as small as required to mitigate the threat model) was intentionally doubled to preclude any chance of false alarm due to the mismatch of receivers, resetting of PRN type biases, and other effects of algorithm tuning. The anomaly on SVN 54 (PRN 18) in 2016 occurred during this transition and may have nearly tripped the SQM threshold had it not been increased. Still, even with this elevated threshold, the dashed blue curve in Figure 2a showed that the largest expected range error at this threshold, pessimistically by the ICAO threat model, is still less than 1.5 meters. And the minimum current error limits for L1 users provide plenty of margin.
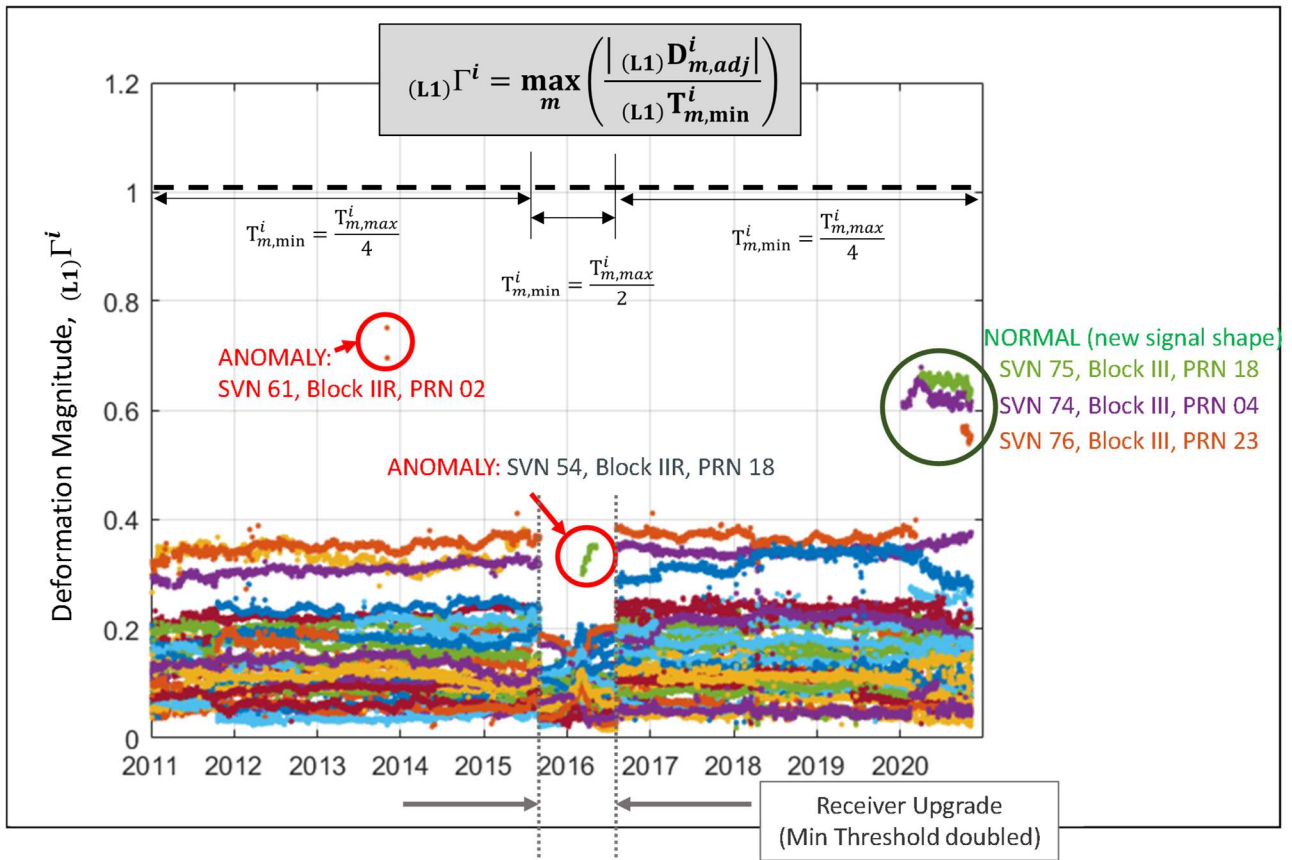

Figure 3. Maximum average detection tests at UDREI=5 for the four current WAAS metrics ($9 \leq m \leq 12$) on L1 for the years 2011 to 2020.

Figure 3 also shows that the nominal monitor biases for GPS-III SVs (i.e., SVN 74 (PRN 04), SVN 75 (PRN 18), and SVN 76 (PRN23)) are consistently elevated despite not resulting from an anomaly. Recall that this is because the monitor is referenced to the median over all satellite signals in view for each metric. (See Equation 11). The Block III SVs likely use more modern

signal generation hardware and techniques [5]. Accordingly, their transmitted codes differ more substantially from those the previous GPS Block types. While likely a better representation of an "ideal" L1 C/A code signal, until enough satellites from this block are included in the navigation solution, they will appear as nominally biased to users. This is expected and acceptable, given the current error limits. Still, offline monitoring and consistency checks continue to be provided on an ongoing basis through the William J. Hughes FAA Technical Center [8]. This monitoring helps to provide confidence that nominal system behavior remains as expected.

Dish Data

In addition, to offline monitoring, large, high-gain, high-resolution dish captures of the signals can sometimes be analyzed [2]. These can be used to form more precise models of the signals to better estimate the true errors from nominal signal deformations. These dish captures provide good insights but are limited in that the data is often not easy to obtain. (It is not possible to be continually logged for multiple SVs simultaneously or continuously nor is the data readily available.)

In addition to the data collected by Stanford (using the SRI dish) in [2], dish collections were also done by MITRE for L5 on the Block IIF SVs in 2016 and by NWIC Pacific (via U.S. Air Force) for a limited subset of SVs on L1 in 2020. These signals are plotted in Figure 4 below.
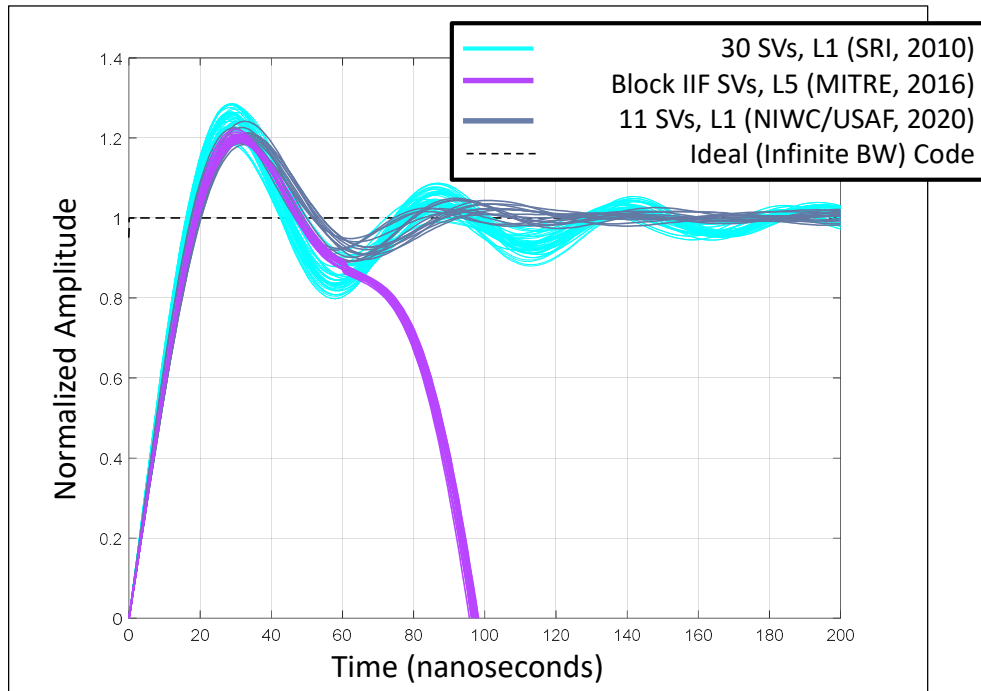

Figure 4. Comparison of code step responses from measurements of GPS signals collected using high-gain, directional dish antennas in 2010 (L1 only, full constellation), 2016 (L5 only, IIF only), and 2020 (L1-only, partial constellation).

The maximum WAAS monitor metrics for each of these three dish signal capture groups are plotted in Figure 5. Note that because the measurements on L1 in 2020 were taken with different equipment than from 2010 and because the subset of SVs differ substantially, the metrics cannot be directly compared for individual SVs. (The median from Equation 11 is not the same for each group.) However, the maximum variation—after median removal—can compared for consistency. With the exception of SVN 62, the variation is limited to within 50% of the minimum threshold for both data groups taken 10 years apart. In addition to the WAAS metric consistency shown in Figure 3, these observations further suggest the maximum nominal range biases on all SVs are also consistent over this time.
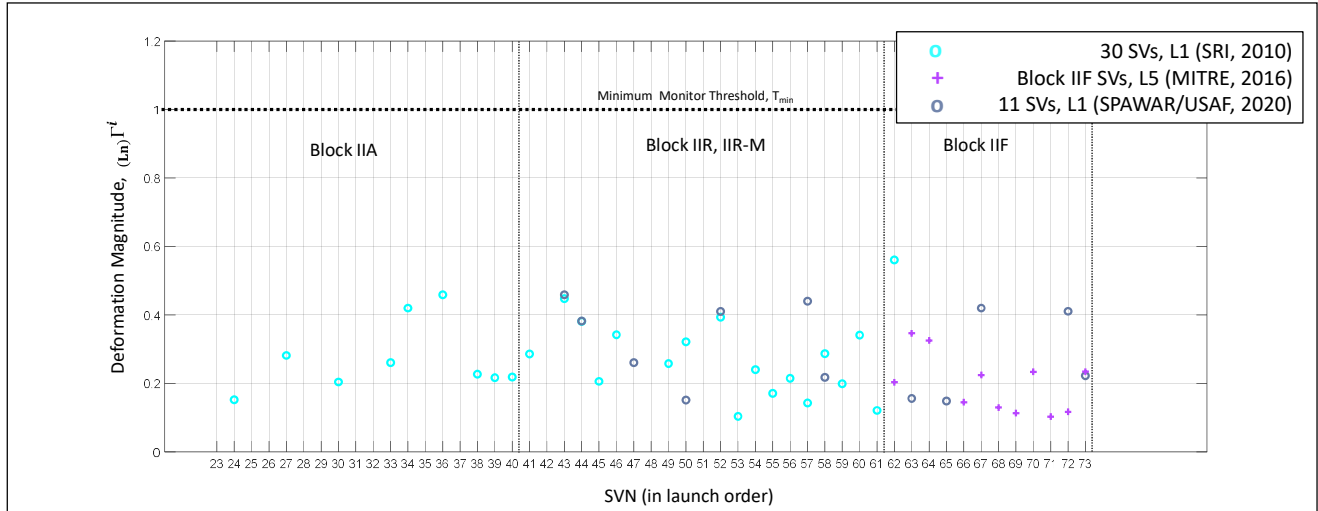
Figure 5. WAAS metrics computed from the signals measured using the high-gain dish collection efforts in 2010, 2016 and 2020. (Only original 4 metrics are used for L1 to correspond to the WAAS data from Figure 3

High-resolution observations of several GPS satellites and signals were also made in 2020 by [12]. They estimated the magnitude of the maximum differential range error on GPS SVs (for the allowed WAAS user receiver configuration of Figure 1a) was estimated at ~50 cm—well below the 1.5 meters modeled by the threat model. For dual-frequency users (or Figure 1b), the estimated maximum range error was estimated at ~15 cm on L1 and ~10 cm on L5.

WAAS SQM NOMINAL DEFORMATION BIASES (2021-)

The stability of nominal biases is established by Figure 3 using the original (4) metrics and the existing WAAS SQM implementation. The new metrics and the L5 signal require additional post processing of the data. Because the L5 algorithms are yet implemented in the operational system however, the real-time metrics are not available for the ~10 years these signals have been online. (In fact, the ground receivers were only capable of processing the L5 signal after 2017.) But given the stability of the nominal performance over the past 10 years—where, with the exception of the Block III SVs, even a single day gives an approximate value for the largest monitor metric over all SVs—a more limited data sample may be sufficiently representative going forward.

Figure 6a plots all 8 chip-shape metrics ($1 \leq m \leq 8$) on L1 for all SVs for a single nominal day (June 30, 2021). Figure 6b plots all 8 chip shape metrics ($1 \leq m \leq 8$) on L5 for the same day. The metrics are normalized by the minimum achievable threshold for each signal. That is, $_{(L1)}T_{m,min} =_{(L1)}T_{m,max}/4$ $_{(L5)}T_{m,min} =_{(L5)}T_{m,max}/1.71$, for L1 and L5 respectively. As with Figure 3, the L1 signals reach between 60-70% of the threshold because the Block III SVs. The L5 metrics also reach between 60-70% of the threshold, however for both Block IIF and Block III SVs, despite a larger minimum threshold.

The nominal biases across metrics appear to limit the minimum detection thresholds more on L5 relative to L1. This is despite the fact that the correlator spacings are similar (~100 ns from early-to late) and comparable (average) spacings of its additional correlator outputs. These levels are tolerable however since $_{(L5)}T_{m,min} =_{(L5)}T_{m,max}/1.71$ meets the threat mitigation/error limit requirement for DFREI = 2. (See Figure 2b.) And this range error limit is satisfactory.

It's possible the relative difference in bias levels indicate differences in how the L5 signal is generated on the satellites relative to L1. Alternatively, the elevated L5 monitor biases could stem from the reduced number of available L5 signals. WAAS observes approximately half the number of L5signals as L1. (See Figure 7.) This may increase the variations in the median operation of Equation (11), leading to inflated nominal biases and noise on each individual metric. This should decrease as additional L5-capable (Block III) satellites come online.
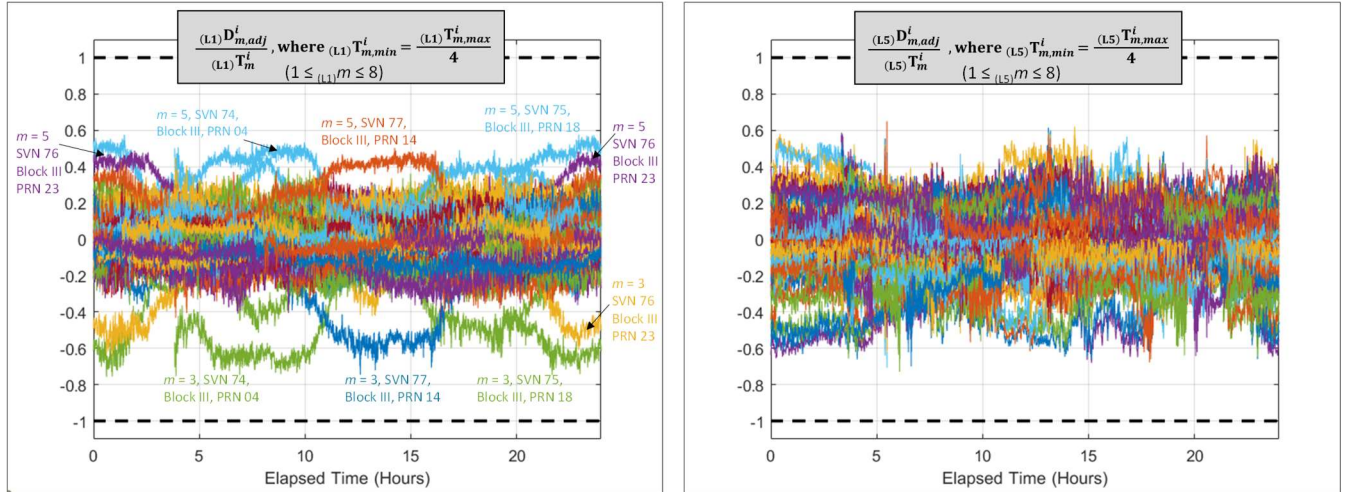
Figure 6a. (Left) L1 normalized chip-shape metrics ($1{\leq}m{\leq}8$) for all GPS SVs on June 30, 2021.
Figure 6b. (Right) L5 normalized chip-shape metrics ($1{\leq}m{\leq}8$) for all GPS SVs on June 30, 2021.
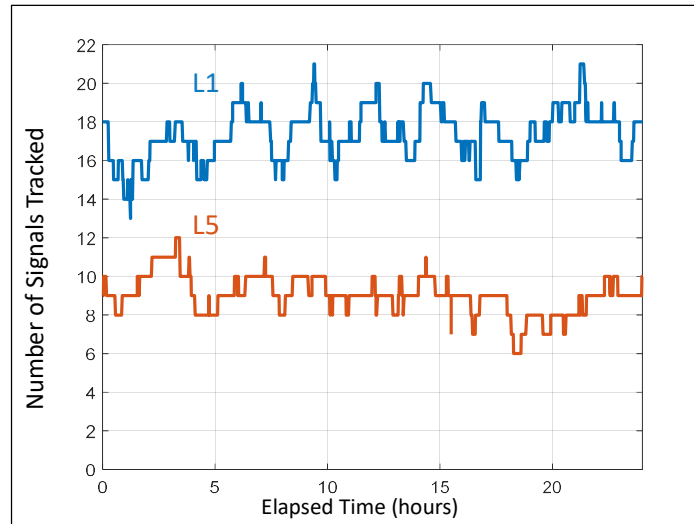

Figure 7. Number of L1 and L5 satellite signals observed on June 30, 2021.

WAAS SQM DEFORMATION ANOMALY EVENT: JULY 1, 2021

It's useful to examine at least one case of an anomalous deformation event in greater detail, where all the metrics—current and proposed—can be compared.

On July 1, 2021 reportedly an unintentional, "off-nominal" configuration of the L1 and L2 signals was broadcast from SVN66- (PRN 27) from 1100 to 2300 UTC. Reportedly several GBAS stations excluded the satellite. For WAAS, one metric—metric 12 of the currently implemented L1 metrics ($9{\leq}m{\leq}12$)—came close to exceeding the threshold. However, no trip occurred.

Figures 8a and 8b below show the metric values—8 proposed chip-shape metrics ($1{\leq}m{\leq}8$) + 4 current ($9{\leq}m{\leq}12$) relative to the threshold. Metric 12 rose above the came close to tripping in but did not. This was also true for the operational system. The chip-shape metrics (7 and 8) also react to this distortion however their thresholds are larger so were ultimately less sensitive to it. (Future tuning of the thresholds may change this.) Had these additional metrics already been implemented in WAAS with ~30% smaller $_{(L1)}T_{min}$ on these metrics, the WAAS SQM may have tripped and set the satellite to "Do Not Use" until the event ended. Figure 9 shows a zoomed in view of these near threshold crossings.
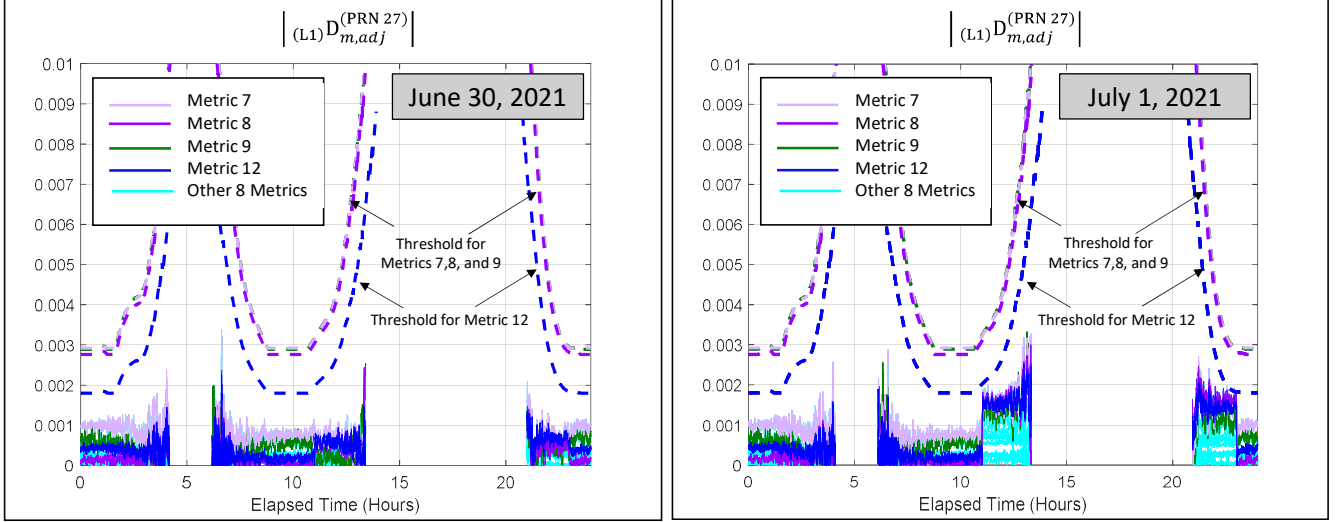
Figure 8a. (Left) L1 chip-shape metrics (1≤*m*≤8) and current metrics (9≤*m*≤12) for SVN 66 (PRN 27) on June 30, 2021.
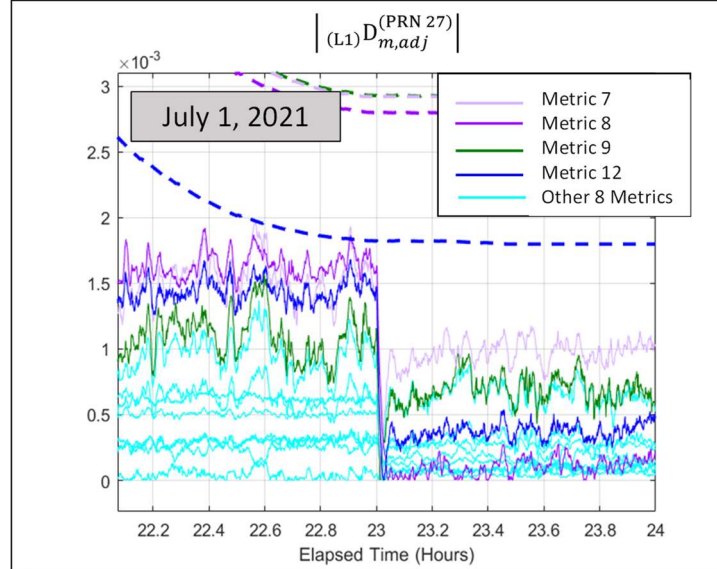**Figure 8b**. (Right) L1 chip-shape metrics (1≤*m*≤8) and current metrics (9≤*m*≤12) for SVN 66 (PRN 27) on June 30, 2021.

Figure 9. Enlarged plot of L1 chip-shape metrics (1≤*m*≤8) and current WAAS metrics (9≤*m*≤12) for SVN 66 (PRN 27) on June 30, 2021

While not shown, there was no noticeable change on L5 during this fault. Its metric behavior remained nominal. This is consistent with the fault assertions that a simultaneous signal deformation fault on L1 and L5 is not expected to occur

CONCLUSIONS

Approximately 10 years of WAAS signal quality monitor data has been analyzed. Numerous algorithm and system improvements have occurred over time and have improved integrity against signal deformations. Assessments of nominal and anomalous deformation magnitudes in the range domain have been consistent with expectations—i.e., they were either well-bounded by the error limits and/or mitigated by the monitor.

The maximum nominal monitor biases on L1 for all GPS SVs are relatively stable over time and remain well below the minimum detection thresholds. This implies they are upper-bounded by 1 to 1.5 meters, assuming faulted conditions. High-

gain dish measurements in [12] estimate that for L1-only users they are likely below 50 cm. And, for dual-frequency users (with a more constrained receiver design space), they are likely consistently at or below 15 cm on L1 and 10 cm on L5.

Monitor processing for the L5 signal is largely the same as for L1, however additional metrics will be added to both L1 and L5 to meet the more-challenging detection requirements for dual-frequency users. The original four detection metrics on L1 continue to be robust and provide integrity for L1 users with low probability of false alarms. But the additional chip-shape metrics also appear to be very sensitive to signal deformations—both nominal and faulted.

As expected, L1 signals from GPS Block III SVs appear less similar to previous block types. The monitor bias reflects that. This will eventually change when a sufficient number of Block III SVs are on orbit. (Over time, L1 signals from fewer remaining SVs will appear more dissimilar, however, until the constellation is more uniform again.) This difference is not as significant for L5, which implies the signal generation hardware for L5 signals is more similar between Block IIF and Block III SVs. However, their monitor biases appear inflated relative to L1, possibly due to fewer available L5 signals at this time. This too should also evolve and improve with increasing number of Block III (L5-capable) SVs.

ACKNOWLEDGMENTS

REFERENCES

1. Shloss, Peter, Phelts, R. Eric, Walter, Todd, Enge, Per, "A Simple Method of Signal Quality Monitoring for WAAS LNAV/VNAV," *Proceedings of the 15th International Technical Meeting of the Satellite Division of The Institute of Navigation (ION GPS 2002)*, Portland, OR, September 2002, pp. 800-808.
2. Phelts, R. Eric, Altshuler, Eric, Walter, Todd, Enge, Per, "Validating Nominal Bias Error Limits Using 4 years of WAAS Signal Quality Monitoring Data," Proceedings of the ION 2015 Pacific PNT Meeting, Honolulu, Hawaii, April 2015, pp. 956-963.
3. Phelts, R.E., *Multicorrelator Techniques for Robust Mitigation of Threats to GPS Signal Quality*, Ph.D. Thesis, 2001, Stanford University, Stanford, CA.
4. Rife, J., Phelts, E., "Formulation of a Time-Varying Maximum Allowable Error for Ground-Based Augmentation Systems," *Proceedings of the 2006 National Technical Meeting of The Institute of Navigation*, Monterey, CA, January 2006, pp. 441-453.
5. Thoelert, Steffen, Steigenberger, Peter, Montenbruck, Oliver, Meurer, Michael, "GPS III Arrived – An Initial Analysis of Signal Payload and Achieved User Performance," *Proceedings of the 32nd International Technical Meeting of the Satellite Division of The Institute of Navigation (ION GNSS+ 2019)*, Miami, Florida, September 2019, pp. 1059-1075.
6. Phelts, R.E., Walter, T., Enge, P., "Toward Real-Time SQM for WAAS: Improved Detection Techniques," *Proceedings of the 16th International Technical Meeting of the Satellite Division of The Institute of Navigation (ION GPS/GNSS 2003)*, Portland, OR, September 2003, pp. 2739-2749.
7. Phelts, R. Eric, Wong, Gabriel, Walter, Todd, Enge, Per, "Signal Deformation Monitoring for Dual-Frequency WAAS," *Proceedings of the 2013 International Technical Meeting of The Institute of Navigation*, San Diego, California, January 2013, pp. 93-106.
8. FAA WAAS PAN Report Archive. https://www.nstb.tc.faa.gov/DisplayArchive.htm
9. Minimum Operational Performance Standards (MOPS) for WAAS, DO-229D. RTCA.
10. Phelts, R. Eric, Walter, Todd, Enge, Per, Akos, Dennis M., Shallberg, Karl, Morrissey, Tom, "Range Biases on the WAAS Geostationary Satellites," *Proceedings of the 2004 National Technical Meeting of The Institute of Navigation*, San Diego, CA, January 2004, pp. 110-120.

11. Shallberg, Karl W., Ericson, Swen D., Phelts, Eric, Walter, Todd, Kovach, Karl, Altshuler, Eric, "Catalog and Description of GPS and WAAS L1 C/A Signal Deformation Events," *Proceedings of the 2017 International Technical Meeting of The Institute of Navigation*, Monterey, California, January 2017, pp. 508-520.
12. Thoelert, Steffen, Circiu, Mihaela-Simona, Meurer, Michael, "Impact of Satellite Biases on the Position in Differential MFMC Applications," *Proceedings of the 2020 International Technical Meeting of The Institute of Navigation*, San Diego, California, January 2020, pp. 222-235